Research Square

Preprints are preliminary reports that have not undergone peer review.
They should not be considered conclusive, used to inform clinical practice,
or referenced by the media as validated information.

Ultrasound-Guided Layered Sacral Canal Injection Determines Epidural Compartmental Drug Delivery: A Fluoroscopic Anatomical Study with Hydrodynamic Analysis

Wenlue Wu
Affiliated Hospital of Guangdong Medical College Hospital
Shuangyun Chen
Affiliated Hospital of Guangdong Medical College Hospital
Xuelian Huang
Chuiliang Liu
lcl1204@aliyun.com
Affiliated Hospital of Guangdong Medical College Hospital
Xiao Wu
Affiliated Hospital of Guangdong Medical College Hospital
Yuehong Ye
Affiliated Hospital of Guangdong Medical College Hospital

Research Article

Keywords: Caudal epidural injection, Ultrasonography, Interventional, Epidural space, Pain Management, Injections, Epidural

Posted Date: November 24th, 2026

DOI: https://doi.org/10.21203/rs.3.rs-11348316/v1

License: This work is licensed under a Creative Commons Attribution 4.0 International License. Read Full License

Additional Declarations: No competing interests reported.

Abstract

Background

Sacral canal injection is widely used in interventional pain management, yet the influence of injection layer on differential drug distribution between the anterior epidural space (AES) and posterolateral epidural spaces (PESs) remains unquantified. This anatomical and hydrodynamic study determines whether ultrasound-guided layer-specific injection governs targeted epidural compartment delivery.

Methods

In this prospective, single-center, assessor- and participant-blinded non-randomized anatomical hydrodynamic study with observational contrast spread measurements, 60 participants were sequentially assigned 1:1:1 to superficial (Group S), middle (Group M), or deep-layer (Group D) injections. Iohexol was injected under ultrasound guidance into the designated layer. Diffusion patterns, cephalad spread, compartmental filling grades, and sacral foraminal leakage grade were recorded via dynamic fluoroscopy. Hydrodynamic analysis focused on the competitive filling relationship between AES and PESs, quantified by multivariable regression to identify independent determinants of cephalad spread.

Results

Group S achieved 90% PESs-targeted success; Group M had 60% bidirectional spread; Group D reached 80% AES-targeted success. Injection layer was negatively correlated with cephalad spread (β=-0.659; 95%*CI* -1.19 to -0.13; P = 0.020); sacral canal diameter was positively correlated with AES-specific spread (β = 3.938; 95%*CI* 1.17 to 6.71; P < 0.001). PESs filling grade was inversely correlated with AES-specific spread (β=-0.758; 95%*CI* -1.26 to -0.26; P < 0.001), confirming a competitive hydrodynamic filling dynamic between compartments. Sacral foraminal leakage grade was negatively correlated with both AES-specific (β=−0.606; 95%*CI* − 0.98 to − 0.23; P = 0.002) and PESs-specific cephalad spread (β=−0.802; 95%*CI* − 1.36 to − 0.24; P = 0.006). Only minor vascular injuries occurred(5%), with no severe adverse events reported.

Conclusions

Ultrasound-guided layered sacral canal injection determines predictable, compartment-targeted drug delivery. Injection layer, sacral canal diameter, compartmental filling grade, and sacral foraminal leakage grade are independent key determinants of cephalad spread. These findings provide an algorithmic technical framework for precision epidural therapy.

Trial registration

Chinese Clinical Trial Registry (ChiCTR2500114729) retrospectively registered on December 17, 2025.

INTRODUCTION

The epidural space is anatomically subdivided into three distinct compartments: the anterior epidural space (AES) and a pair of posterolateral epidural spaces (PESs)[1]. Sacral canal injection, a well-established technique widely used in interventional pain management, relies on the targeted diffusion within specific epidural compartments to achieve therapeutic efficacy. Although ultrasound-guided sacral canal injection has been shown to improve procedural success rates (96.9%–100%) and significantly reduce intravascular injection incidence (0%–3.2%), the directional diffusion patterns of injectate from the sacral canal into specific epidural compartments remain inadequately characterized[2–5].

Prior ultrasound-guided caudal injection studies confirmed procedural feasibility and safety[2–5], but none differentiated injectate distribution between the AES and PESs, and none quantified the correlation between needle depth and compartment-specific targeting. Consequently, the critical question of whether injection layer governs directional epidural diffusion has remained unanswered.

Based on prior clinical anatomical observations, we hypothesized that the proposed “layered sacral canal injection” framework (Fig. 1) would determine epidural diffusion: superficial-layer injections would predominantly diffuse within the PESs, middle-layer injections would lead to bidirectional AES/PESs diffusion, and deep-layer injections would primarily target the AES. We therefore designed this non-therapeutic interventional anatomical and hydrodynamic methodological study with observational fluoroscopic outcome measurements to determine whether ultrasound-guided layered sacral injection enables targeted epidural compartment delivery, and to identify hydrodynamic factors influencing cephalad spread, thereby establishing a standardized anatomical and methodological basis for targeted epidural drug delivery.

MATERIALS AND METHODS

Study design and patients

This prospective, single-center, assessor- and participant-blinded, non-randomized, non-therapeutic interventional anatomical and hydrodynamic methodological study with observational fluoroscopic outcome assessments was conducted at our institution between June and October 2024 in accordance with the Declaration of Helsinki, with ethical approval granted by the Ethics Committee of Foshan Fosun Chancheng Hospital (**No. CYEC-LCYJ-2024009-PJ-20240229**). Written informed consent to participate was obtained from all participants before enrollment. The study was voluntarily retrospectively registered in the Chinese Clinical Trial Registry (registration number: **ChiCTR2500114729**) on December 17, 2025, with the date of first patient enrollment being July 9, 2024 and the link to the trial's registration documents available at https://www.chictr.org.cn/. Imaging evaluators and data statisticians remained fully blinded to group allocation throughout the study; all participants were also blinded to group assignment; only the procedural anesthesiologist could not be blinded due to the technical nature of layered injection and the need for real-time ultrasound-guided needle localization.

As this was an exploratory study with no prior quantitative data on compartment-specific delivery rates, a formal power-based sample size calculation was not performed. The target sample size (n = 60, 20 per group) was determined a priori based on feasibility, precision of proportion estimates, and exploratory-study convention, with a 15% allowance for post-enrollment exclusion. The primary endpoint for sample size consideration was the PESs-targeted delivery success rate, and a 25% absolute difference was prespecified as

the minimum clinically meaningful difference based on clinical judgment; this threshold was not used for formal power computation. AES-targeted and bidirectional-targeted success rates were treated as secondary endpoints. Eligible participants were consecutively allocated 1:1:1 to Groups S, M, and D, and excluded cases were replaced to maintain 20 valid datasets per group (Fig. 2).

Inclusion criteria: age 18–65 years, ASA I or II, BMI 18.0–30.0 kg/m², no history of chronic low back pain or lumbar disc herniation. Exclusion criteria: history of lumbosacral spine surgery, allergy to local anesthetics/iodinated contrast agents, severe cognitive impairment, contraindication to sacral puncture, or pregnancy/lactation. Post-enrollment exclusion criteria: inadequate ultrasound visualization of sacral hiatus anatomy, sacral canal diameter < 0.2 cm, ambiguous needle tip placement, poor imaging resolution, or incidental lumbar disc herniation on contrast imaging.

Ultrasound scanning, layer localization and injection protocol

Ultrasound scanning, layer localization and injection protocol
All procedures were performed by an attending physician with > 5 years of experience in ultrasound-guided regional anesthesia, using a 6–13 MHz high-frequency linear array transducer (Sonosite X-Porte). Participants were positioned with a pelvic tilt pad for optimal sacrococcygeal exposure. Standardized anatomical measurements of the sacral hiatus were performed via ultrasound (Fig. 3): coronal view for sacral cornua distance (s), longitudinal view for sacral canal anteroposterior diameter (d) and sacral hiatus length (l), with identification of core landmarks including the posterior sacrococcygeal ligament (L) and deep sacrococcygeal ligament (d-L).

All injections were performed with a 22G × 80 mm nerve stimulation needle under ultrasound guidance on the longitudinal sacral hiatus plane, with standardized layer localization: Group S injection site was the fluid plane deep to the posterior sacrococcygeal ligament via hydrodissection (Fig. 1); Group M site was the fluid plane within the central sacral canal soft tissue, without contact with the sacrococcygeal ligaments (Fig. 1); Group D site was the fluid plane anterior to the deep sacrococcygeal ligament (Fig. 1).

The contrast solution was 20 mL of 150 mg I/mL iohexol dilution. A 5-mL initial bolus was administered at 0.25–0.33 mL/s, followed by fluoroscopy to confirm epidural distribution and exclude intravascular/intrathecal injection. The remaining 15 mL was administered via the same pulsed technique over 45–60 seconds, with standard anteroposterior (AP) and lateral (Lat) lumbosacral radiographs acquired within 5 minutes of injection completion.

Outcome Measures

Primary outcomes: distribution of epidural diffusion patterns, and target compartment delivery success rate. Diffusion patterns were classified as exclusive PESs diffusion, exclusive AES diffusion, bidirectional diffusion (simultaneous PESs and AES spread), and no cephalad diffusion (contrast confined to the sacral canal without extension above S1). PESs-targeted success was defined as exclusive PESs or bidirectional diffusion; AES-targeted success was defined as exclusive AES or bidirectional diffusion; bidirectional-targeted success was defined as simultaneous spread in both compartments.

Secondary outcomes: cephalad spread segments above S1 (overall on AP views, AES/PESs-specific on Lat views); AES and PESs compartmental filling grade (0–3 scale, graded on Lat views by contrast width to intervertebral foramen height ratio, Fig. 4: Grade 0 = no visible contrast medium; Grade 1 = ratio ≤ 1/4; Grade 2 = ratio > 1/4 and ≤ 1/2; Grade 3 = ratio > 1/2. AG1-3 represent AES grades 1–3, and PG1-3 represent PESs grades 1–3); sacral foraminal leakage grade (0–3 scale, graded on AP views by leakage band number and density, Fig. 5: Grade 0 = no leakage bands; Grade 1 = ≤ 3 light grey leakage bands; Grade 2 = > 3 light grey leakage bands or ≤ 3 dark grey leakage bands; Grade 3 = > 3 dark grey leakage bands or ≥ 1 dense black band); compartment-specific iohexol cephalad diffusion intensity visualized via heatmap analysis (Fig. 6); and procedure-related adverse events (monitored intraprocedurally and at 24-hour follow-up). All imaging outcomes were assessed as observational fluoroscopic measurements of contrast distribution patterns, without evaluation of therapeutic efficacy endpoints.

Statistical Analysis

Statistical analyses were performed using SPSS 26.0 software, with a two-sided $P < 0.05$ defined as statistically significant. Normally distributed continuous data were presented as mean ± standard deviation (SD), and categorical variables as frequencies (n, %). One-way ANOVA with post-hoc Tukey test was used for intergroup comparisons of continuous data; Pearson chi-square test was applied for bilateral diffusion rate analysis, two-sided Fisher's exact test for categorical variables with frequencies, and Bonferroni-corrected Fisher's exact test (adjusted $\alpha = 0.0167$) for post-hoc pairwise comparisons of categorical variables. Spearman rank correlation was used for ordinal variables and continuous cephalad spread segments, and Pearson correlation for normally distributed continuous variables. Multivariable linear regression models were built for three prespecified outcomes (overall cephalad spread on anteroposterior views, AES/PESs-specific spread on lateral views) to identify independent influencing factors; candidate variables were prespecified per anatomical and hydrodynamic theory, with variables of univariate $P < 0.1$ retained and non-qualified prespecified confounders excluded. Hydrodynamic analysis specifically quantified the competitive filling relationship between AES and PESs compartments using multivariable regression modeling.

RESULTS

A total of 60 eligible participants (20 per group) with complete procedural and imaging datasets were ultimately included in the final statistical analysis, with the full participant screening, enrollment, group allocation and exclusion flow detailed in the STROBE-compliant Fig. 2.

Baseline demographic and anatomical characteristics of the included participants are summarized in Table 1. No statistically significant intergroup differences were observed in baseline demographic and anatomical characteristics (all $P > 0.05$), with BMI showing a borderline between-group difference ($P = 0.050$). The potential confounding effect of BMI was controlled via the prespecified variable inclusion rule in the multivariable regression model.

Table 1
Baseline demographic and anatomical characteristics (n = 20 per group)

Age (year)		**Group S**	**Group M**	**Group D**	**P-value**
		40.3 ± 11.5	**38.8 ± 10.0**	**37.1 ± 10.1**	**0.645[a]**
Gender					0.502[c]
	male	14 (70%)	10 (50%)	13 (65%)	
	female	6 (30%)	10 (50%)	7 (35%)	
BMI (kg/m²)		23.4 ± 2.6	22.4 ± 2.9	24.6 ± 2.8	0.051 [a]
Sacral cornua distance 's' (cm),		1.8 ± 0.3	1.8 ± 0.4	1.8 ± 0.3	0.982 [a]
Sacral canal diameter 'd' (cm),		0.6 ± 0.1	0.6 ± 0.2	0.6 ± 0.2	0.394 [a]
Sacral hiatus length 'l' (cm),		2.6 ± 0.9	2.8 ± 0.9	2.8 ± 0.9	0.778 [a]
a: One-way analysis of variance (ANOVA); c: Pearson chi-square test					

Primary Outcome: Compartment-Specific Diffusion Patterns

Significant layer-specific directional diffusion was observed across the three groups, confirming that ultrasound-guided layered injection determines targeted epidural compartment delivery ($P < 0.001$, Table 2). Group S showed predominant diffusion in the PESs with a PESs-targeted delivery success rate of 90%, Group M achieved the highest bidirectional diffusion rate (60%) with a PESs-targeted success rate of 95%, and Group D exhibited predominant AES diffusion with an AES-targeted delivery success rate of 80%.

Table 2
Distribution of epidural diffusion patterns and target compartment delivery success rates among the three groups (n = 20 per group)

	Group S	Group M	Group D	P value	Pairwise comparison P value		
					S vs M	S vs D	M vs D
Diffusion pattern				< 0.001[a]	-	-	-
Exclusive PESs diffusion	9 (45%)	7 (35%)	0 (0%)				
Exclusive AES diffusion	0 (0%)	0 (0%)	9 (45%)				
Bidirectional diffusion (PESs + AES)	9 (45%)	12 (60%)	7 (35%)				
No cephalad diffusion	2 (10%)	1 (5%)	4 (20%)				
Targeted delivery success rate							
PESs-targeted delivery success	18 (90%)	19 (95%)	7 (35%)	< 0.001[b]	1.000[c]	< 0.001[c]	< 0.001[c]
AES-targeted delivery success	9 (45%)	12 (60%)	16 (80%)	0.074[b]	0.342[c]	< 0.001[c]	0.168[c]
Bidirectional targeted delivery success	9 (45%)	12 (60%)	7 (35%)	0.280[b]	0.342[c]	0.519[c]	0.113[c]
a: Two-sided Fisher's exact test for the 4-category diffusion pattern distribution (R×C contingency table)							
b: Two-sided Fisher's exact test for overall between-group comparisons of binary targeted delivery success rates							
c: Pairwise comparisons were performed using Fisher's exact test with Bonferroni correction							

Pairwise comparisons with Bonferroni correction were performed for the primary endpoint of PESs-targeted success rate (overall $P < 0.001$), revealing that the PESs-targeted success rates of Group S and Group M were significantly higher than that of Group D (both $P < 0.001$), with no significant difference between Group S and Group M ($P = 1.000$). For AES-targeted delivery success rate, no statistically significant difference was found among the three groups in the overall omnibus test ($P = 0.070$), though Group D showed a trend towards higher AES targeting efficiency. For diffusion patterns on AP radiographs, 100% of patients in Group M and Group D presented bilateral diffusion, while 95% of patients in Group S showed bilateral diffusion, with no unilateral diffusion observed in the middle- and deep-layer injection groups (Fig. 5).

Secondary Outcomes

Further quantitative analysis of diffusion characteristics revealed significant intergroup differences in cephalad spread, compartmental filling grades, and foraminal leakage (Table 3). On AP views, Group D had significantly fewer overall cephalad diffusion segments compared with Group S and Group M ($P < 0.001$). A significant between-group difference was observed in the rate of no cephalad diffusion (Fisher's exact test, $P = 0.019$), with Group D showing a markedly higher no-diffusion rate (40%) than Group S (10%) and Group M (5%). On lateral radiograph views, Group S and Group M had significantly more PESs-specific cephalad spread segments than Group D ($P < 0.001$), with no intergroup difference in AES-specific spread ($P = 0.660$). Consistently, Group S and Group M had significantly higher PESs filling grades than Group D ($P < 0.001$), with no significant difference in AES filling grade across groups ($P = 0.100$). For sacral foraminal leakage, Group M had the lowest mean leakage grade, followed by Group S and Group D, with a significant between-group difference ($P = 0.002$).

Table 3. Diffusion characteristics, associated factors and multivariable regression of iohexol after layered sacral canal injection(n=20 per group)

Panel A Comparison of diffusion characteristics among three groups

	Group S	Group M	Group D	P *value*
Anteroposterior view				
Bilateral diffusion, n (%)	19 (95)	20 (100)	20 (100)	1.000[c]
No cephalad diffusion, n (%)	2 (10)	1 (5)	8 (40)	0.019[b]
Cephalad diffusion segment	2.3 ± 1.7	2.5 ± 1.2	0.9 ± 1.1	**0.001**[a]
Foraminal leakage grade	1.4 ± 1.0	0.8 ± 1.0	2.0 ± 1.0	**0.002**[a]
Lateral view				
AES-specific diffusion segments	1.7 ± 2.3	2.3 ± 2.4	1.9 ± 1.6	0.663[a]
PESs-specific diffusion segments	4.0 ± 3.4	4.2 ± 2.0	1.3 ± 1.9	**0.001**[a]
AES compartmental filling grade	0.5 ± 0.6	0.7 ± 0.7	1.0 ± 0.7	0.100[a]
PESs compartmental filling grade	1.5 ± 0.9	1.9 ± 1.0	0.4 ± 0.6	**< 0.001**[a]

Panel B Association of leakage/filling grade with cephalad diffusion and adverse events

	Group S, n (%)	Group M, n (%)	Group D, n (%)	Cephalad diffusion segments	P *value*
Foraminal leakage grade					
Grade 0	6 (30)	12 (60)	1 (5)	2.5 ± 1.5	**0.001**[a]
Grade 1	4 (20)	2 (10)	7 (35)	1.8 ± 1.6	
Grade 2	7 (35)	5 (25)	3 (15)	2.4 ± 1.4	
Grade 3	3 (15)	1 (5)	9 (45)	0.5 ± 0.5	
AES compartmental filling grade					**< 0.001**[a]
Grade 0	11(55)	8(40)	4(20)	0	
Grade 1	8(40)	10(50)	14(70)	3.0 ± 1.9	
Grade 2	1(5)	2(10)	1(5)	4.5 ± 1.3	
Grade 3	0	0	1(5)	2.0 ± 0	
PESs compartmental filling grade					**< 0.001**[a]
Grade 0	2(10)	1(5)	13(65)	0	
Grade 1	10(50)	9(45)	6(30)	3.9 ± 1.9	
Grade 2	5(25)	2(10)	1(5)	4.3 ± 1.5	
Grade 3	3(15)	8(40)	0	5.1 ± 3.6	
Procedure-related adverse events	0	1(5)	2(10)		**0.766**[b]

Panel C Multivariable linear regression analyses of influencing factors for cephalad diffusion

Variable	AP diffusion segments			Lat-AES diffusion segments			Lat-PESs diffusion segments		
	β (95% CI)	SE	^{m}P	β (95% CI)	SE	^{m}P	β (95% CI)	SE	^{m}P
Constant	-9.116 (-36.76, 18.53)	13.742	0.510	6.724 (-21.20, 34.65)	13.880	0.630	17.60 (-23.99, 59.19)	20.673	0.399
Injection layer*	**-0.659 (-1.19, -0.13)**	0.262	**0.015**	-0.509 (-1.04, 0.02)	0.265	0.061	-0.361 (-1.16, 0.43)	0.395	0.365
Sacral canal diameter 'd' **(cm)**	2.042 (-0.70, 4.78)	1.363	0.141	**3.938 (1.17, 6.71)**	1.377	**0.006**	0.187 (-3.94, 4.31)	2.051	0.928
Foraminal leakage grade	-0.268 (-0.64, 0.10)	0.185	0.154	**-0.606 (-0.98, -0.23)**	0.187	**0.002**	**-0.802 (-1.36, -0.24)**	0.279	**0.006**
AES compartmental filling grade	0.154 (-0.46, 0.76)	0.303	0.614	**1.704 (1.09, 2.32)**	0.306	**<0.001**	0.714 (-0.20, 1.63)	0.456	0.124
PESs compartmental filling grade	0.217 (-0.28, 0.71)	0.245	0.378	**-0.758 (-1.26, -0.26)**	0.247	**0.004**	**1.222 (0.48, 1.96)**	0.368	**0.002**

Table notes

a: One-way analysis of variance (ANOVA) for overall intergroup comparison of continuous variables.

b: Two-sided Fisher's exact test.

c: Pearson chi-square test for overall intergroup comparison.

*Injection layer coding: superficial-layer = 1, middle-layer = 2, deep-layer = 3.

Abbreviations: AES = anterior epidural space; PESs = posterior epidural space; AP = anteroposterior; Lat = lateral; SE = standard error; **mP = P-value for multivariable regression model**.

To further visually validate the layer-specific directional diffusion characteristics, we performed compartment-specific iohexol cephalad diffusion intensity heatmap analysis (Fig. 6). The heatmap visually confirmed our core hypothesis: superficial-layer injection yielded the strongest cephalad diffusion in the PESs, deep-layer injection achieved the most extensive spread in the AES, and middle-layer injection presented balanced bidirectional diffusion in both compartments—providing intuitive visual evidence for the hydrodynamic mechanism of layer-dependent compartmental diffusion.

Correlation analysis further clarified the relationship between diffusion parameters and cephalad spread (Table 3, Panel B), showing that sacral foraminal leakage grade was negatively correlated with cephalad spread segments ($P < 0.001$), while compartmental filling grade was positively correlated with spread in the corresponding compartment ($P < 0.001$ for both AES and PESs). Multivariable linear regression was subsequently performed to identify independent determinants of iohexol cephalad spread (Table 3, Panel C). Injection layer was negatively correlated with overall AP cephalad diffusion (β = -0.659; 95% *CI* -1.19 to -0.13; P = 0.015), sacral canal diameter was positively correlated with AES-specific spread (β = 3.938; 95% *CI* 1.17 to

6.71; *P* = 0.006), and leakage grade was negatively correlated with spread in both compartments (all *P* < 0.001). Notably, PESs filling grade was inversely correlated with AES-specific diffusion (β = -0.758; 95% *CI* -1.26 to -0.26; *P* = 0.004), indicating competitive hydrodynamic filling between the two epidural compartments.

No severe adverse events occurred during the procedure or 24-hour follow-up. Only 3 cases of minor transient vascular injury with self-limiting intraoperative bleeding were reported, with no hematoma, intravascular/intrathecal injection, neurological deficit or allergic reaction observed. The incidence of procedure-related adverse events was 0 in Group S, 5% (1/20) in Group M and 10% (2/20) in Group D, with no significant between-group difference (*P* = 0.766, Table 3, Panel B).

DISCUSSION

This ultrasound-guided layered sacral canal injection study establishes and validates a standardized framework that determines predictable, compartment-specific directional injectate spread within the epidural space. Our core findings confirm that superficial-layer injections predominantly target the PESs, middle-layer injections yield balanced bidirectional AES/PESs coverage, and deep-layer injections preferentially target the AES. Through systematic hydrodynamic analysis, we further identified four independent determinants of cephalad spread and described a novel competitive filling dynamic between the AES and PESs, providing the first quantitative anatomical and hydrodynamic basis for precision epidural therapy via sacral canal injection.

Our core findings align with and substantially extend seminal prior studies in this field. Doo et al.[5] previously demonstrated that ultrasound-guided superficial-layer injection improved caudal block success and reduced intravascular injection risk; our study builds on this foundational work by further quantifying the 90% PESs-targeting accuracy of superficial-layer injection, and for the first time characterizing the compartment-specific diffusion profile of this approach in vivo. Park et al.[4] reported that needle insertion depth affects overall epidural spread in caudal injection, but their work did not differentiate injectate distribution between the AES and PESs; our study fills this critical gap by defining the three-layer anatomical division of the sacral canal, and systematically quantifying how each injection layer determines directional diffusion in distinct epidural compartments. The anatomical basis of our model is further corroborated by the work of Hüppe et al.[1], who characterized the PESs as the primary low-resistance flow pathway in the sacral epidural space. The intact posterior sacrococcygeal ligament and midline dorsal fibrous structures act as physical barriers to restrict anterior injectate migration, which directly explains the high PESs-targeting specificity of superficial-layer injection observed in our study.

The primary innovation of this study is the first establishment of a three-layer anatomical and functional division of the sacral canal injection space, with systematic quantification of layer-specific directional diffusion in the AES and PESs. Previous studies were limited to binary comparisons of procedural outcomes between superficial and deep needle placement, without subdividing the sacral canal into functionally distinct layers or differentiating injectate distribution between the ventral and dorsal epidural compartments. Our three-layer injection model transforms the decades-old conventional empiric caudal injection—long plagued by inconsistent drug distribution and unpredictable therapeutic efficacy—into a precision-targeted intervention with predictable compartment-specific delivery.

A second key, paradigm-shifting novel finding of this study is the competitive hydrodynamic filling dynamic between the AES and PESs. Our multivariable regression analysis demonstrated that PESs filling grade was inversely correlated with AES-specific diffusion, providing the first in vivo quantitative evidence that the low-resistance PESs acts as the preferential flow pathway for injectate in the sacral epidural space. Only when the PESs is fully saturated can injectate migrate into the higher-resistance AES. This finding aligns with the pressure gradient principles described in prior epidural hydrodynamic studies by Blomberg and Savolaine[7,8], but extends this prior work by establishing a direct, quantitative competitive relationship between the two epidural compartments. Critically, this finding overturns the long-held empiric clinical belief that increasing injection volume is the primary strategy to improve AES spread[9]; instead, our data demonstrate that direct deep-layer injection to bypass the PESs preferential filling effect is the most reliable method for targeted AES delivery.

We further identified previously unreported, compartment-specific determinants of cephalad spread[10]. Specifically, we found that sacral canal diameter was an independent positive predictor of AES cephalad spread but had no significant impact on PESs spread, a finding that aligns with the narrow, enclosed anatomical structure of the AES[11] and is further explained by the competitive filling dynamic we identified. We also quantified the independent effects of injection layer, sacral foraminal leakage grade, and compartmental filling grade on longitudinal injectate spread, and established the first compartment-specific predictive model of epidural diffusion. This model supplements and refines the classical epidural hydrodynamics theory, which has historically been limited to global spread prediction[12,13]. Notably, the low-speed pulsed injection protocol adopted in this study effectively controlled the confounding effect of injection speed on diffusion, and minimized sacral foraminal leakage by maintaining stable epidural pressure homeostasis, which is consistent with the hydrodynamic principles verified by Bosscher et al.[12].

These layer-specific findings have direct technical implications for clinical practice. Superficial-layer injection is preferred when the therapeutic target is confined to the PESs—for example, in posterior epidural adhesions or sacral radiculopathy—as it achieves 90% PESs-targeting accuracy with minimal AES diversion and is suitable for novice operators[14]. Middle-layer injection offers the optimal risk-benefit profile for diffuse lumbosacral pain requiring dual-compartment coverage, such as multilevel spinal stenosis, providing the highest bidirectional diffusion rate, the lowest foraminal leakage, and the maximal cephalad spread. Deep-layer injection is recommended when AES delivery is essential—for instance, in ventral disc herniation-related discogenic pain or anterior epidural pathology—as it is the most reliable method to bypass the preferential PESs filling effect, despite a higher sacral foraminal leakage risk[6,15]. This stratified approach allows operators to select the injection depth based on preprocedural lesion localization and therapeutic goals, offering an immediate, zero-cost refinement to routine practice.

This study has several limitations. First, the single-center design and moderate sample size may limit generalizability, requiring multicenter validation. Second, the 150 mgI/mL iohexol used provided limited AES/PESs boundary delineation on AP views, with potential minor grading bias; future studies may optimize contrast concentration or use CT imaging to enhance resolution. Additionally, foraminal leakage was assessed only at the sacral foramina, not at the lumbar intervertebral foramina, because the injection was delivered into the sacral canal and the primary hydrodynamic endpoints were compartmental AES/PESs targeting and cephalad epidural spread. Although lumbar foraminal spread is clinically relevant for radicular pain, dedicated lumbar-level assessment was beyond the scope of this anatomical hydrodynamic study. Future studies should

incorporate lumbar foraminal contrast grading and correlate it with clinical outcomes. Third, this study was conducted in participants without spinal pathological lesions, and diffusion patterns may differ in patients with epidural adhesion or spinal stenosis. Finally, we did not correlate diffusion patterns with long-term clinical pain outcomes, requiring future prospective studies to confirm therapeutic efficacy in specific pain populations.

CONCLUSION

Ultrasound-guided layered sacral canal injection determines precise, compartment-specific directional drug diffusion in the epidural space. Injection layer, sacral canal diameter, compartmental filling grade, and sacral foraminal leakage grade are independent key determinants of cephalad spread. This hydrodynamic analysis provides a novel methodological and anatomical theoretical framework, as well as a standardized practical algorithm, for precision interventional pain management.

Abbreviations

AES
anterior epidural space
PESs
posterolateral epidural spaces
AP
anteroposterior
Lat
lateral
ASA
American Society of Anesthesiologists
BMI
body mass index
CI
confidence interval
SD
standard deviation
SE
standard error
CT
computed tomography
MRI
magnetic resonance imaging
STROBE
Strengthening the Reporting of Observational Studies in Epidemiology
AG
anterior epidural space grade
PG
posterolateral epidural space grade

mP
P value for the multivariable regression model.

Declarations

Ethics approval and consent to participate

The study was conducted in accordance with the Declaration of Helsinki and was approved by the Ethics Committee of Foshan Fosun Chancheng Hospital (No. CYEC-LCYJ-2024009-PJ-20240229). Written informed consent to participate was obtained from all participants before enrollment.

Consent for publication

Not applicable.

Availability of data and materials

The datasets generated and analyzed during the current study are available from the corresponding author upon reasonable request.

Competing Interests

The authors declare no conflicts of interest.

Funding

This work was supported by the 2025 Foshan Science and Technology Program (No. 2420001004082), the 2025 Internal Research Project of Foshan Fosun Chancheng Hospital (No. FX2025010), and the Foshan Municipal Health Commission Medical Scientific Research Project (No. 202632021002). The funders had no influence on the study design, data collection and analysis, decision to publish, or preparation of the manuscript.

Authors' contributions

WW and CL conceived and designed the study. WW, SC, XH, XW and YY performed the procedures and acquired the data. SC, XH and XW analyzed and interpreted the data. WW drafted the manuscript. CL and YY critically revised the manuscript. All authors read and approved the final manuscript.

Acknowledgements

We thank all the patients who participated in this study.

References

1. Hüppe T, Pattar G, Maass B. Caudal Anesthesia: Overview and Practical Recommendations. Anasthesiol Intensivmed Notfallmed Schmerzther, 2022; 57(11-12): 724-736.

2. Klocke R, Jenkinson T, Glew D. Sonographically guided caudal epidural steroid injections. J Ultrasound Med, 2003; 22:1229–1232.
3. Oh D. The Influence of Ultrasound-Guided Technique Using a Catheter-Over-Needle on the Incidence of Accidental Intravascular Injection during Caudal Block-A Retrospective Case Series Study. Medicina (Kaunas), 2021; 57(4): 318.
4. Park SJ, Yoon KB, Shin DA, et al. Influence of needle-insertion depth on epidural spread and clinical outcomes in caudal epidural injections: A randomized clinical trial. J Pain Res. 2018, 11, 2961-2967.
5. Doo AR, KIM JW, LEE JH, et al. A comparison of two techniques for ultrasound-guided caudal injection: The influence of the depth of the inserted needle on caudal block. Korean J Pain, 2015, 28(2): 122-128.
6. Nakahashi M, Uei H, Hoshino M, et al. Anatomical Evaluation of the Sacral Hiatus Using Ultrasound Imaging: Factors That Inhibit Needle Insertion During Caudal Epidural Block Procedures. Pain Pract. 2020; 20(1):55-61.
7. Blomberg RG, Olsson SS. The lumbar epidural space in patients examined with epiduroscopy. Anesth Analg. 1989;68(2): 157-160.
8. Savolaine ER, Pandya JB, Greenblatt SH, et al. Anatomy of the human lumbar epidural space: new insights using CT-epidurography. Anesthesiology. 1988; 68(2):217-220.
9. Kim KM, Kim HS, Choi KH, et al. Cephalic spreading levels after volumetric caudal epidural injections in chronic low back pain. J Korean Med Sci. 2001; 16(2): 193-197.
10. Lundblad M, Eksborg S, Lönnqvist PA. Secondary spread of caudal block as assessed by ultrasonography. Br J Anaesth. 2012; 108(4): 675-681. doi: 10.1093/bja/aer513.
11. Boezaart AP, Prats-Galino A, Nin OC, et al. The Posterior Lumbar Epidural Space: Three-Dimensional Reconstruction of High-Resolution MRI: Real and Potential Epidural Spaces and Their Content In Vivo. Pain Med. 2019; 20(9): 1687-1696.
12. Bosscher H. Pressure-Volume Relationships in the Spinal Canal and Potential Neurological Complications After Epidural Fluid Injections. Front Pain Res (Lausanne). 2022; 3: 884277.
13. Hong JH, Jung SW, Park JH. The Effect of Speed of Normal Saline Injection on Optic Nerve Sheath Diameter in Thoracic Epidural Anesthesia. Pain Physician. 2019; 22(4): E325-E332.
14. Ma D, Chen P, Xu J. Learning curve of ultrasound-guided caudal epidural block: a CUSUM pivotal analysis. Front Med (Lausanne). 2025; 12: 1624205.
15. Kanai A, Suzuki A, Hoka S. Rapid injection of epidural mepivacaine speeds the onset of nerve blockade. Can J Anaesth. 2005; 52(3): 281-284.

Figures

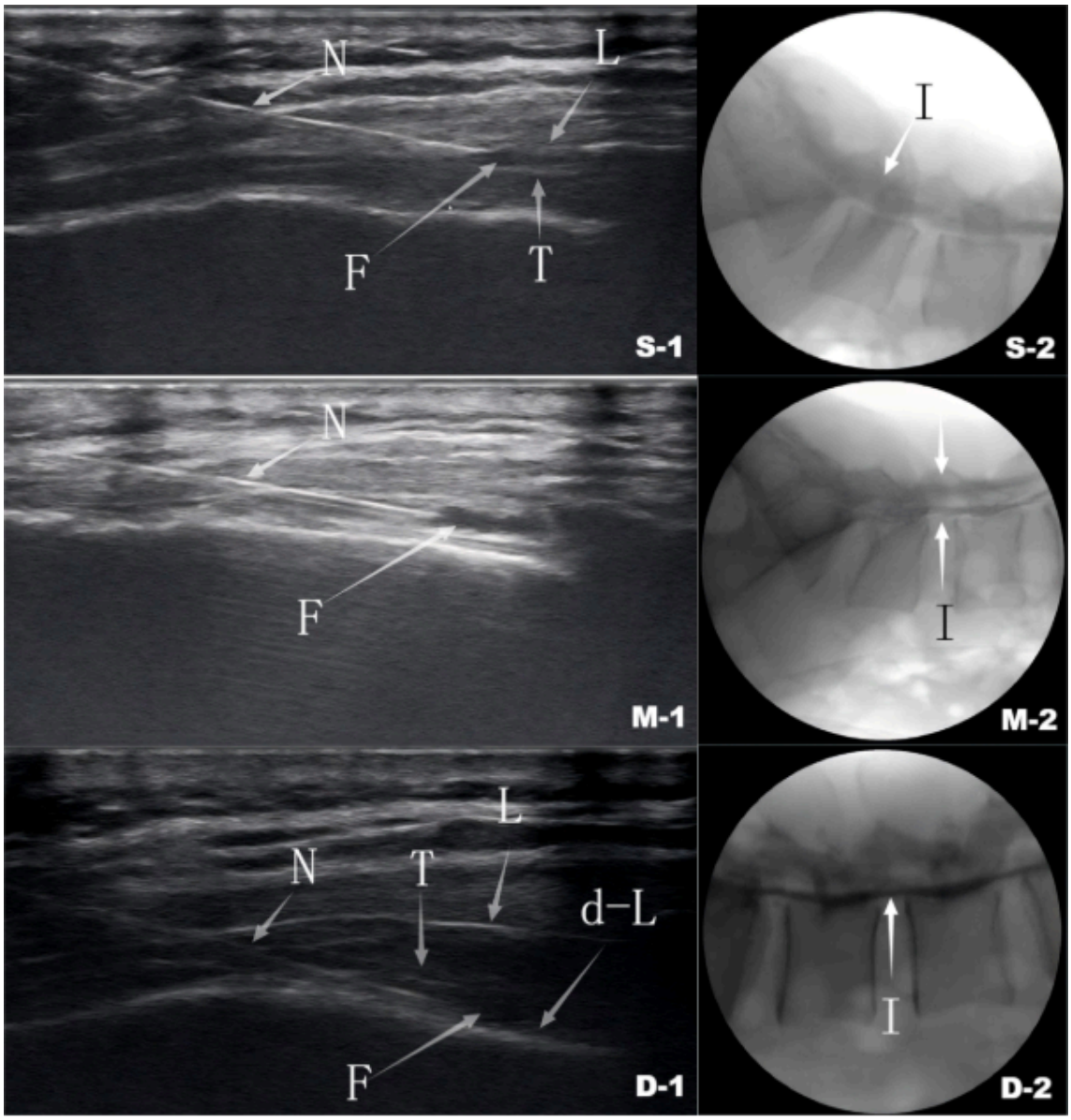


Figure 1

Schematic representation of the ultrasound-guided layered sacral canal injection model. Panels S-1, M-1, D-1 display ultrasound images for superficial-, middle-, and deep-layer injections, respectively. S-2: fluoroscopy showing contrast diffusion in posterolateral epidural spaces after superficial-layer injection; M-2: bidirectional contrast spread in anterior and posterolateral epidural spaces following middle-layer injection; D-2: predominant contrast distribution within the anterior epidural space after deep-layer injection

Abbreviations: N = nerve stimulation needle; L = posterior sacrococcygeal ligament; d-L = deep sacrococcygeal ligament; F = fluid plane; T = soft tissue within the sacral canal; I = iohexol dilution

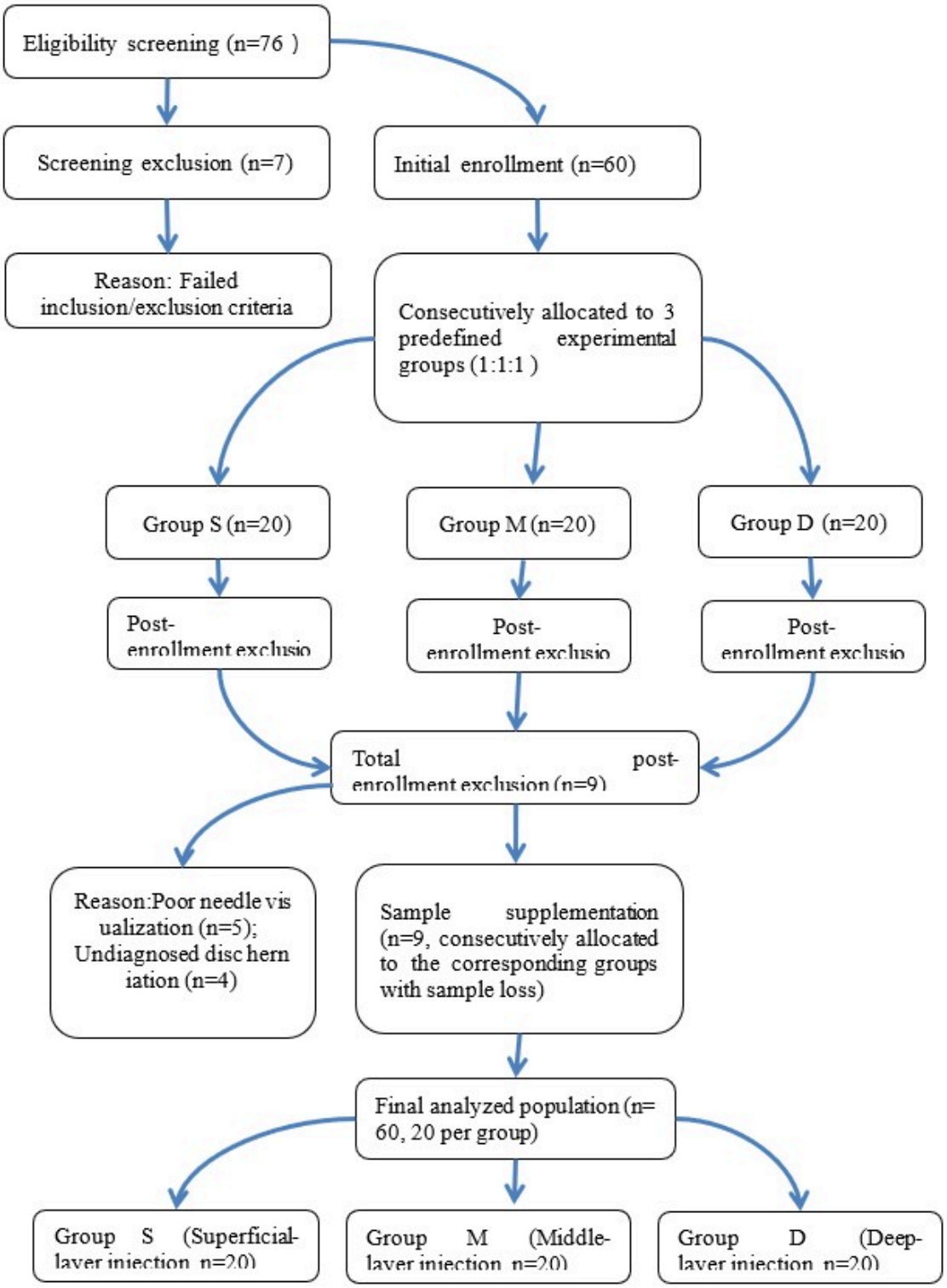


Figure 2

Study flow diagram of participant screening, enrollment, group allocation and final analysis

Abbreviations: S = superficial-layer injection group; M = middle-layer injection group; D = deep-layer injection group

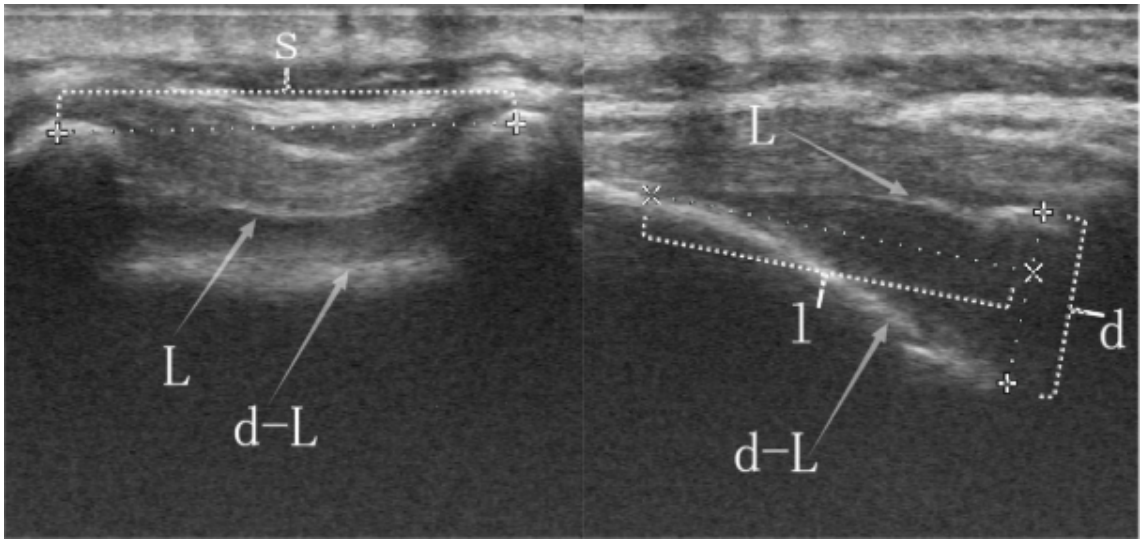


Figure 3

Ultrasound imaging of the sacral hiatus region and standardized anatomical measurement parameters

Abbreviations: s = distance between the midpoints of the bilateral sacral cornua; d = maximum anteroposterior diameter of the sacral canal; l = distance from the superior edge of the sacral hiatus to the ligamentous junction; L = posterior sacrococcygeal ligament; d-L = deep sacrococcygeal ligament

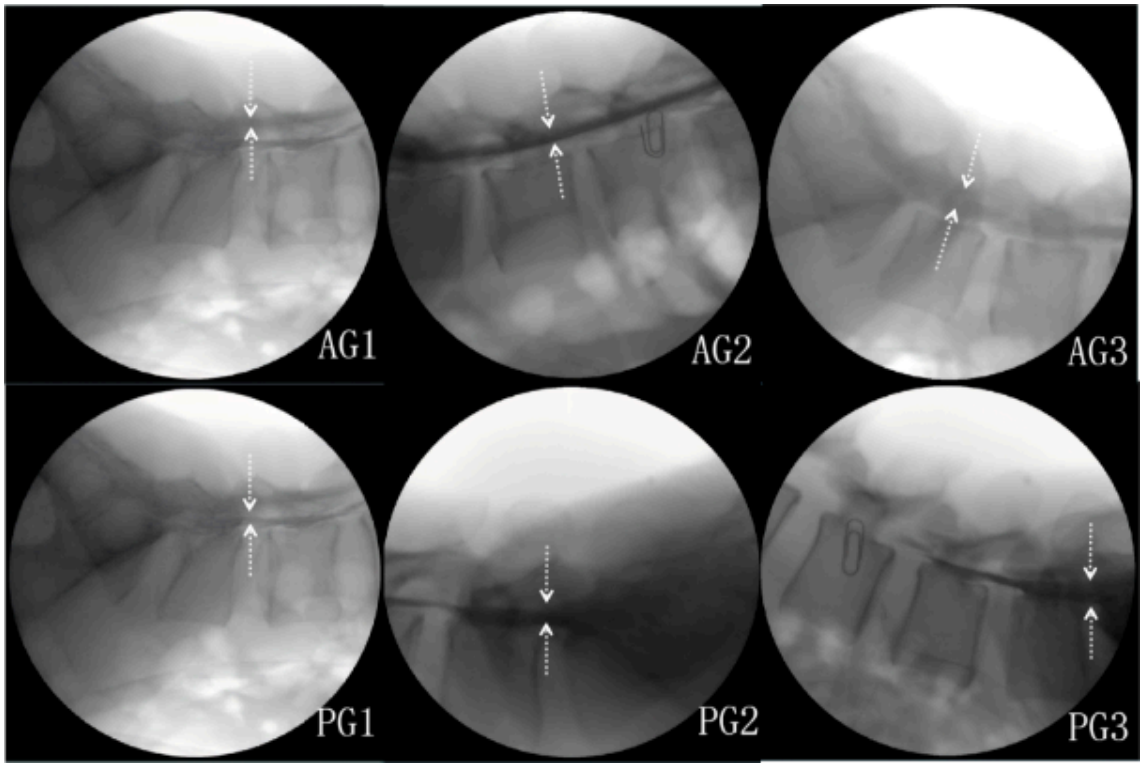


Figure 4

Grading standard for epidural space contrast filling on lateral lumbar radiographs

Abbreviations: AES = anterior epidural space; PESs = posterolateral epidural spaces; AG1-3 = AES grades 1–3; PG1-3 = PESs grades 1–3.

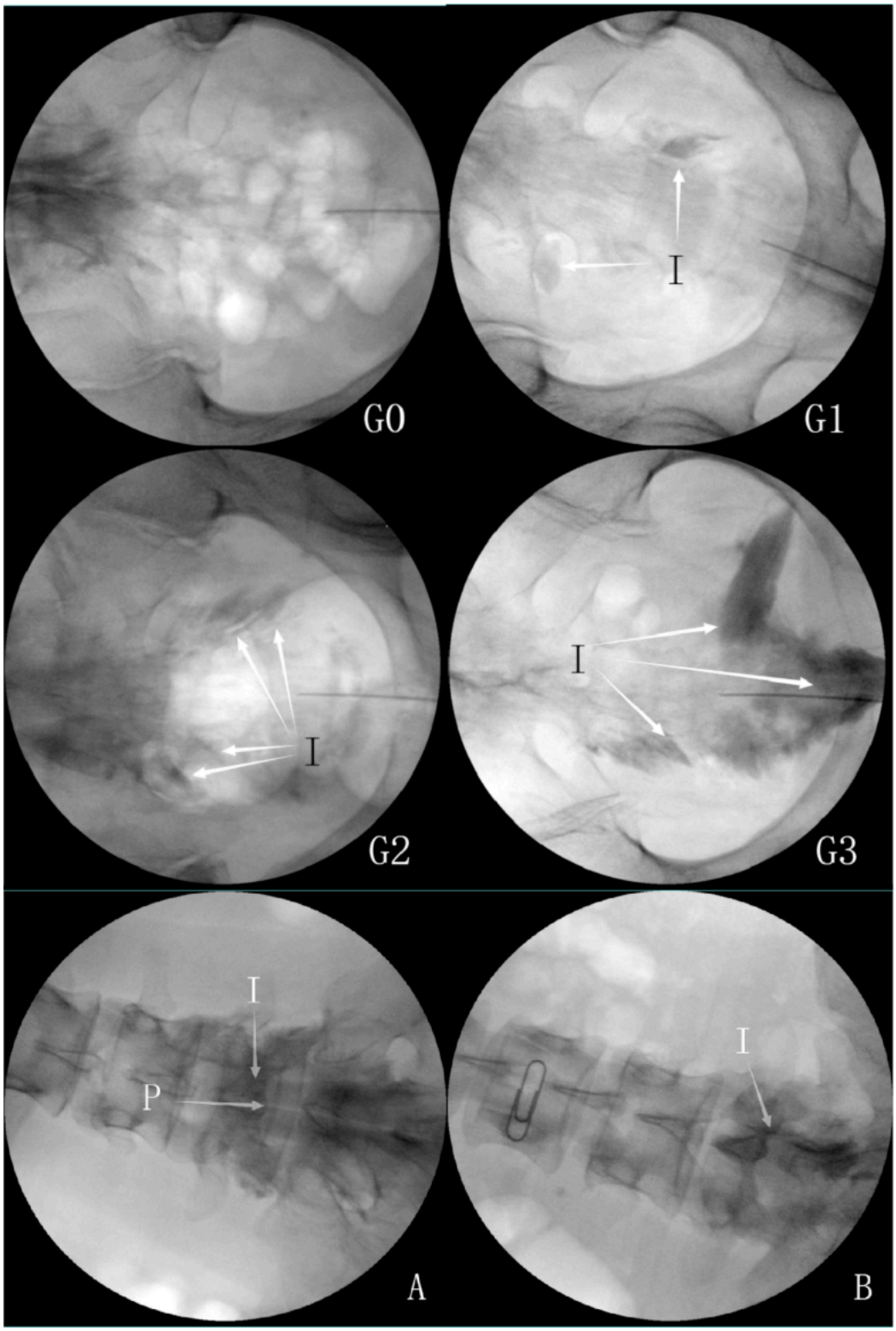


Figure 5

Grading standard for sacral foramina contrast leakage on AP views. Panels A and B demonstrate representative contrast-diffusion patterns in the posterolateral epidural space: A, bilateral spread; B, right-sided spread.

Abbreviations: G = sacral foramina contrast-leakage grade (G0-G3 represent grades 0-3); I = iohexol dilution.

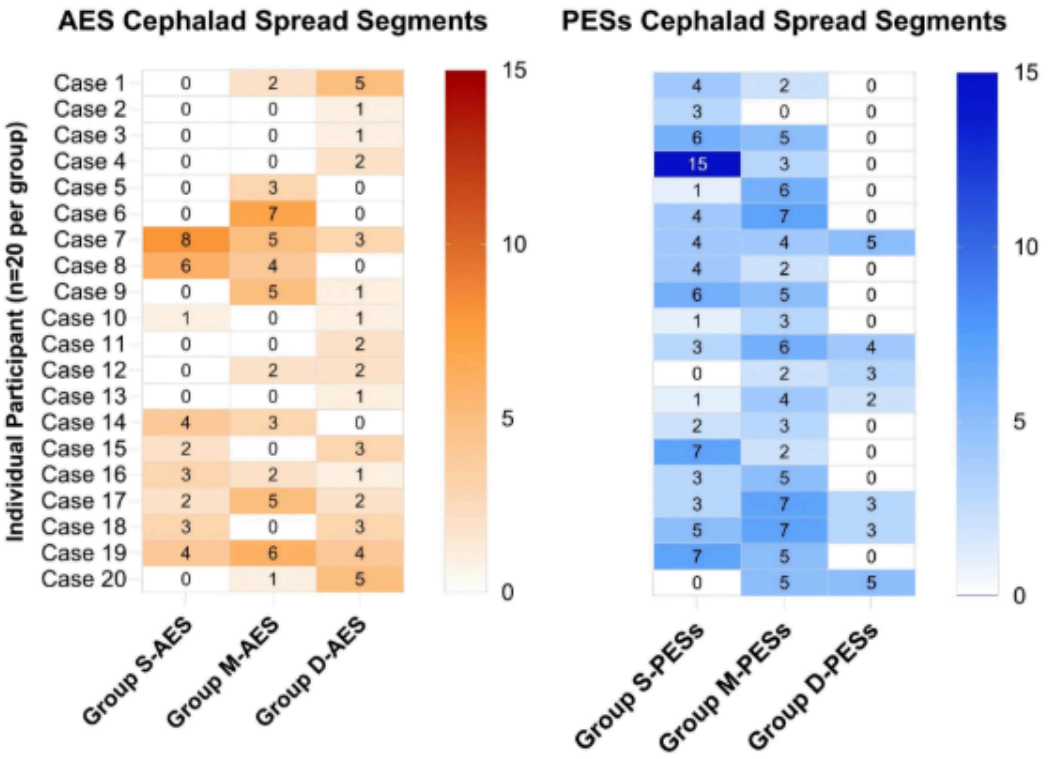


Figure 6

Heatmap of compartment-specific iohexol cephalad diffusion intensity across 60 included participants.

Abbreviations: S = superficial-layer injection group; M = middle-layer injection group; D = deep-layer injection group; AES = anterior epidural space; PESs = posterolateral epidural spaces.